HOW TO MOBILIZE MMWAVE: A JOINT BEAM AND CHANNEL TRACKING APPROACH

Jiahui Li[†]*, Yin Sun*[§]*, Limin Xiao*[‡¶]*, Shidong Zhou*[†]*, Ashutosh Sabharwal*[*]

[†]Dept. of EE, [‡]Research Institute of Information Technology, Tsinghua University, Beijing, 100084, China
[§]Dept. of ECE, Auburn University, Auburn AL, 36849, U.S.A.
[*]Dept. of ECE, Rice University, Houston TX, 77251, U.S.A.

ABSTRACT

Maintaining reliable millimeter wave (mmWave) connections to many fast-moving mobiles is a key challenge in the theory and practice of 5G systems. In this paper, we develop a new algorithm that can jointly track the beam direction and channel coefficient of mmWave propagation paths using phased antenna arrays. Despite the significant difficulty in this problem, our algorithm can simultaneously achieve fast tracking speed, high tracking accuracy, and low pilot overhead. In static scenarios, this algorithm can converge to the minimum Cramér-Rao lower bound of beam direction with high probability. Simulations reveal that this algorithm greatly outperforms several existing algorithms. Even at SNRs as low as 5dB, our algorithm is capable of tracking a mobile moving at an angular velocity of 5.45 degrees per second and achieving over 95% of channel capacity with a 32-antenna phased array, by inserting only 10 pilots per second.

Index Terms— Beam and channel tracking, fast tracking speed, high accuracy, mmWave, phased antenna arrays.

1. INTRODUCTION

Millimeter-wave (mmWave) communication is promising to support the vastly growing data traffic for future wireless systems [1–3]. In the mmWave band, only several distinctive propagation paths exist, i.e., the line-of-sight path and a few relatively strong reflected paths [4, 5]. Therefore, the directional beamforming with large antenna arrays is necessary to provide sufficiently strong received signal power.

To overcome the hardware limitation on the number of radio frequency (RF) chains with large array size and high carrier frequency, analog beamforming with phased antenna arrays was proposed [3, 6–9]. A phased array can receive the signal that is projected onto a certain spatial subspace, with a cost of requiring much more pilots than the fully digital arrays to find the rare and precious paths. When users move quickly, it is needed to track the dynamic paths and even more pilots are required. Hence, one fundamental challenge is how to accurately track a large number of dynamic paths from many high-mobility terminals/reflectors using limited pilots, e.g., in V2V/V2I, high-speed railway, and UAV scenarios [10].

The compressed sensing based algorithms (e.g., [11–13]) were proposed for phased arrays, which can reduce pilot overhead and make beam direction acquisition faster. However, these algorithms are designed for static or quasi-static scenarios, and will encounter performance deterioration under high-mobility scenarios. To cope with high-mobility scenarios, the algorithms in [14–16] use the prior information to track the dynamic beam directions. However, these solutions do not optimize the tracking scheme with the optimal training beamforming vectors, which leads to poor tracking accuracy.

Since the tracking of a large number of dynamic paths can be decoupled into tracking each path with low pilot overhead, we have proposed a beam tracking algorithm in [17, 18] to optimize both the training beamforming vectors and tracking scheme. However, it assumes known channel coefficients, while both channel coefficient and beam direction might be unknown and time-varying in a real mobile system. In this paper, we further develop a recursive beam and channel tracking (RBCT) algorithm to jointly track the dynamic beam direction and channel coefficient. In static scenarios, the Cramér-Rao lower bound (CRLB) of beam direction is derived, which is a function of the training beamforming vectors. We also obtain the *minimum* CRLB by optimizing these training beamforming vectors, and establish three theorems to verify that the RBCT algorithm can converge to the *minimum* CRLB with high probability. Simulations reveal that the RBCT algorithm can achieve much faster tracking speed, lower tracking error, and lower pilot overhead than several existing algorithms.

2. SYSTEM MODEL

Consider a phased array in Fig. 1, where M omnidirectional antennas are placed on a line, with a distance d between two neighboring antennas. Each antenna is connected through a phase shifter to the same RF chain. In time-slot n, the pilot symbols arrive at the array from an angle-of-arrival (AoA) $\theta_n \in [-\frac{\pi}{2}, \frac{\pi}{2}]$. The channel vector is given by

$$\mathbf{h}_n = \beta_n \mathbf{a}(x_n), \tag{1}$$

where $x_n = \sin(\theta_n)$ is the sine of the AoA θ_n, $\mathbf{a}(x_n) = \left[1, e^{j\frac{2\pi d}{\lambda}x_n}, \cdots, e^{j\frac{2\pi d}{\lambda}(M-1)x_n}\right]^{\mathrm{H}}$ is the steering vector of the

¶Corresponding author.

J. Li, L. Xiao, and S. Zhou were supported in part by National S&T Major Project grant 2017ZX03001011-002, National Natural Science Foundation of China grant 61631013, National High Technology Research and Development Program of China (863 Program) grant 2014AA01A703, Science Fund for Creative Research Groups of NSFC grant 61621091, Tsinghua University Initiative Scientific Research grant 2016ZH02-3, International Science and Technology Cooperation Program grant 2014DFT10320, 2011 Plan Wireless Communication Technology Co-Innovation Center grant 20161210020, Tsinghua-Qualcomm Joint Research Program. Y. Sun was supported in part by ONR grant N00014-17-1-2417. A. Sabharwal was supported in part by NSF grants CNS-1518916 and CNS-1314822.

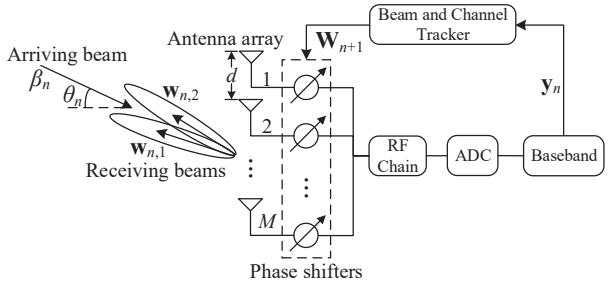

Fig. 1. System model.

arriving beam, λ is the wavelength, and $\beta_n = \beta_n^{\text{re}} + j\beta_n^{\text{im}}$ is the complex channel coefficient.

To track the beam direction x_n and channel coefficient β_n simultaneously, at least two observations using different beamforming vectors are needed. Hence, we assume that two pilot symbols are applied in each time-slot. To receive the i-th ($i = 1, 2$) pilot symbol, let $\mathbf{w}_{n,i}$ be the **beamforming vector** in time-slot n, denoted by

$$\mathbf{w}_{n,i} = \frac{\mathbf{a}(x_n + \delta_{n,i})}{\sqrt{M}}, \tag{2}$$

which is assumed to have the same form as the steering vector. Combining the output signals of the phase shifters yields

$$y_{n,i} = \mathbf{w}_{n,i}^{\text{H}} \mathbf{h}_n s + z_{n,i} = \beta_n \mathbf{w}_{n,i}^{\text{H}} \mathbf{a}(x_n) s + z_{n,i}, \tag{3}$$

where s is the pilot symbol that is known by the receiver, and $z_{n,i} \sim \mathcal{CN}(0, \sigma_0^2)$ is an *i.i.d.* circularly symmetric complex Gaussian random variable. Given $\boldsymbol{\psi}_n = [\beta_n^{\text{re}}, \beta_n^{\text{im}}, x_n]^{\text{T}}$ and $\mathbf{W}_n = [\mathbf{w}_{n,1}, \mathbf{w}_{n,2}]$, the conditional probability density function of $\mathbf{y}_n = [y_{n,1}, y_{n,2}]^{\text{T}}$ is given by

$$p(\mathbf{y}_n | \boldsymbol{\psi}_n, \mathbf{W}_n) = \frac{1}{\pi^2 \sigma_0^4} e^{-\frac{\left\| \mathbf{y}_n - s\beta_n \mathbf{W}_n^{\text{H}} \mathbf{a}(x_n) \right\|_2^2}{\sigma_0^2}}. \tag{4}$$

A beam and channel tracker determines the **beamforming matrix** $\mathbf{W}_n$, and provides an estimate $\hat{\boldsymbol{\psi}}_n = [\hat{\beta}_n^{\text{re}}, \hat{\beta}_n^{\text{im}}, \hat{x}_n]^{\text{T}}$ of the channel coefficient β_n and the sine x_n of the AoA. Let $\xi = (\mathbf{W}_1, \mathbf{W}_2, \ldots, \hat{\boldsymbol{\psi}}_1, \hat{\boldsymbol{\psi}}_2, \ldots)$ be a **beam and channel tracking policy**. In particular, we consider the set Ξ of *causal* beam and channel tracking policies: The estimate $\hat{\boldsymbol{\psi}}_n$ of time-slot n and the beamforming matrix $\mathbf{W}_{n+1}$ of time-slot $n+1$ are determined by using the history of beamforming matrices $(\mathbf{W}_1, \ldots, \mathbf{W}_n)$ and channel observations $(\mathbf{y}_1, \ldots, \mathbf{y}_n)$.

3. BEAM AND CHANNEL TRACKING PROBLEM

Our goal is to develop a joint beam and channel tracking algorithm to minimize the beam tracking error. For any time-slot n, the joint beam and channel tracking problem is given by

$$\begin{aligned} \min_{\xi \in \Xi} \ & \mathbb{E}\left[(\hat{x}_n - x_n)^2 \right] \\ \text{s.t. } & \mathbb{E}\left[\hat{\beta}_n \right] = \beta_n, \ \mathbb{E}\left[\hat{x}_n \right] = x_n, \end{aligned} \tag{5}$$

where the constraint ensures that $\hat{\boldsymbol{\psi}}_n = [\hat{\beta}_n^{\text{re}}, \hat{\beta}_n^{\text{im}}, \hat{x}_n]^{\text{T}}$ is an *un-biased* estimate of $\boldsymbol{\psi}_n = [\beta_n^{\text{re}}, \beta_n^{\text{im}}, x_n]^{\text{T}}$.

Problem (5) is a constrained sequential control and estimation problem that is difficult to solve optimally, where the beamforming matrix $\mathbf{W}_n$ is the control action. First, the system is only partially observed through the channel observation $\mathbf{y}_n$. Second, both the beamforming matrix $\mathbf{W}_n$ and the estimate $\hat{\boldsymbol{\psi}}_n$ need to be optimized: On the one hand, the optimization of $\mathbf{W}_n$ is a non-convex optimization problem of $\delta_{n,i}$ in (2), which is discussed in Section 3.1. On the other hand, as will be discussed in Section 5, the optimization of $\hat{\boldsymbol{\psi}}_n$ is also non-convex and has multiple local optimal estimates.

3.1. Cramér Rao Lower Bound of Beam Tracking

Now, we try to establish a lower bound of the mean square error (MSE) in (5) in *static* scenarios, where the ground true of beam direction and channel coefficient is invariant for all time-slot n, i.e., $\boldsymbol{\psi}_n = [\beta^{\text{re}}, \beta^{\text{im}}, x]^{\text{T}} \triangleq \boldsymbol{\psi}$. Given the beamforming matrices $(\mathbf{W}_1, \ldots, \mathbf{W}_n)$ of the first n time-slots, the MSE in (5) is lower bounded by the CRLB as follows [19]:

$$\mathbb{E}\left[(\hat{x}_n - x)^2 \right] \geq \left[\left(\sum_{i=1}^{n} \mathbf{I}(\boldsymbol{\psi}, \mathbf{W}_i) \right)^{-1} \right]_{3,3}, \tag{6}$$

where $[\cdot]_{i,k}$ obtains the matrix element in row i and column k, and $\mathbf{I}(\boldsymbol{\psi}, \mathbf{W}_i)$ is the 3×3 Fisher information matrix, i.e., [20]

$$\begin{aligned} \mathbf{I}(\boldsymbol{\psi}, \mathbf{W}_i) &\triangleq \mathbb{E}\left[\frac{\partial \log p(\mathbf{y}_i | \boldsymbol{\psi}, \mathbf{W}_i)}{\partial \boldsymbol{\psi}} \cdot \frac{\partial \log p(\mathbf{y}_i | \boldsymbol{\psi}, \mathbf{W}_i)}{\partial \boldsymbol{\psi}^{\text{T}}} \right] \\ &= \frac{2|s|^2}{\sigma_0^2} \begin{bmatrix} \|\mathbf{g}_i\|_2^2 & 0 & \text{Re}\left\{ \mathbf{g}_i^{\text{H}} \mathbf{e}_i \right\} \\ 0 & \|\mathbf{g}_i\|_2^2 & \text{Im}\left\{ \mathbf{g}_i^{\text{H}} \mathbf{e}_i \right\} \\ \text{Re}\left\{ \mathbf{g}_i^{\text{H}} \mathbf{e}_i \right\} & \text{Im}\left\{ \mathbf{g}_i^{\text{H}} \mathbf{e}_i \right\} & \|\mathbf{e}_i\|_2^2 \end{bmatrix}, \end{aligned} \tag{7}$$

where $\mathbf{g}_i = \mathbf{W}_i^{\text{H}} \mathbf{a}(x)$, $\mathbf{e}_i = \beta \mathbf{W}_i^{\text{H}} \dot{\mathbf{a}}(x)$, and $\dot{\mathbf{a}}(x) \triangleq \frac{\partial \mathbf{a}(x)}{\partial x}$. By optimizing the beamforming matrices $(\mathbf{W}_1, \ldots, \mathbf{W}_n)$ on the RHS of (6), we obtain the *minimum* CRLB as below:

$$\begin{aligned} \left[\left(\sum_{i=1}^{n} \mathbf{I}(\boldsymbol{\psi}, \mathbf{W}_i) \right)^{-1} \right]_{3,3} &\geq \min_{\mathbf{W}_1, \ldots, \mathbf{W}_n} \left[\left(\sum_{i=1}^{n} \mathbf{I}(\boldsymbol{\psi}, \mathbf{W}_i) \right)^{-1} \right]_{3,3} \\ &= \min_{\mathbf{W}_i} \frac{1}{n} \left[\mathbf{I}(\boldsymbol{\psi}, \mathbf{W}_i)^{-1} \right]_{3,3}, \end{aligned} \tag{8}$$

where because the linear additive property of Fisher information matrix [20], the optimal $\mathbf{W}_1, \ldots, \mathbf{W}_n$ are the same, and from (7), we can get

$$\left[\mathbf{I}(\boldsymbol{\psi}, \mathbf{W}_i)^{-1} \right]_{3,3} = \frac{\sigma_0^2}{2|s\beta|^2} \cdot \frac{\|\mathbf{g}_i\|_2^2}{\|\mathbf{g}_i\|_2^2 \|\mathbf{e}_i\|_2^2 - \left| \mathbf{g}_i^{\text{H}} \mathbf{e}_i \right|^2}. \tag{9}$$

Problem (8) is non-convex with respect to $\delta_{i,1}$ and $\delta_{i,2}$, which makes it too hard to obtain the analytical solution. However, we can still use the numerical method to find the solution, which yields the optimal beamforming matrix $\mathbf{W}^*$ as below:

$$\mathbf{W}^* = \frac{1}{\sqrt{M}} \left[\mathbf{a}(x - \delta^*), \mathbf{a}(x + \delta^*) \right], \tag{10}$$

where $\delta^* \xrightarrow{M \to \infty} \frac{2\lambda}{3Md}$, and when $M \geq 8$, δ^* is very close to $\frac{2\lambda}{3Md}$. In Fig. 2, the optimal receiving beam directions are depicted by plotting $\frac{1}{[\mathbf{I}(\boldsymbol{\psi}, \mathbf{W}_i)^{-1}]_{3,3}}$ vs. $\delta_{i,1}$ and $\delta_{i,2}$, where $M = 32$, $d = 0.5\lambda$, and the signal-to-noise ratio (SNR) $\frac{|s\beta|^2}{\sigma_0^2}$ is 5dB. It can be observed that δ^* is almost the same as $\frac{2\lambda}{3Md}$ and there are two symmetric optimal solutions. Therefore, we will set $\delta^* = \frac{2\lambda}{3Md}$ in the proposed RBCT algorithm in Section 4.

$$\hat{\boldsymbol{\psi}}_n = \hat{\boldsymbol{\psi}}_{n-1} - \frac{a_n}{\|s\hat{\mathbf{g}}_n\|_2^2\,(l_n^2-|c_n|^2)} \cdot \begin{bmatrix} l_n^2-\mathrm{Im}\{c_n\}^2 & \mathrm{Re}\{c_n\}\,\mathrm{Im}\{c_n\} & -\|\hat{\mathbf{g}}_n\|_2^2\,\mathrm{Re}\{c_n\} \\ \mathrm{Re}\{c_n\}\,\mathrm{Im}\{c_n\} & l_n^2-\mathrm{Re}\{c_n\}^2 & -\|\hat{\mathbf{g}}_n\|_2^2\,\mathrm{Im}\{c_n\} \\ -\|\hat{\mathbf{g}}_n\|_2^2\,\mathrm{Re}\{c_n\} & -\|\hat{\mathbf{g}}_n\|_2^2\,\mathrm{Im}\{c_n\} & \|\hat{\mathbf{g}}_n\|_2^4 \end{bmatrix} \cdot \begin{bmatrix} \mathrm{Re}\{s^{\mathrm{H}}\hat{\mathbf{g}}_n^{\mathrm{H}}(\mathbf{y}_n - s\hat{\beta}_{n-1}\hat{\mathbf{g}}_n)\} \\ \mathrm{Im}\{s^{\mathrm{H}}\hat{\mathbf{g}}_n^{\mathrm{H}}(\mathbf{y}_n - s\hat{\beta}_{n-1}\hat{\mathbf{g}}_n)\} \\ \mathrm{Re}\{s^{\mathrm{H}}\hat{\mathbf{e}}_n^{\mathrm{H}}(\mathbf{y}_n - s\hat{\beta}_{n-1}\hat{\mathbf{g}}_n)\} \end{bmatrix}. \quad (13)$$

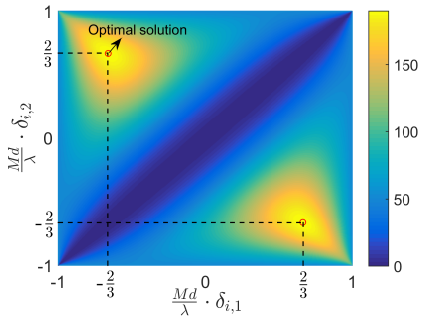

Fig. 2. Optimization of Problem (8) using numerical method.

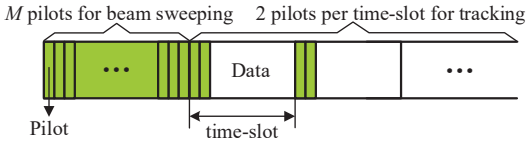

Fig. 3. Frame structure.

4. RECURSIVE BEAM AND CHANNEL TRACKING

We propose a two-stage algorithm to approach the minimum CRLB in (8), which is given below:

Recursive Beam and Channel Tracking (RBCT):

1) Coarse Beam Sweeping: M pilots are used successively (see Fig. 3). The beamforming vector to receive the m-th observation $\tilde{y}_m$ is set as $\tilde{\mathbf{w}}_m = \frac{1}{\sqrt{M}}\mathbf{a}\left(\frac{2m}{M} - \frac{M+1}{M}\right), m = 1,\ldots,M$. Obtain the initial estimate $\hat{\boldsymbol{\psi}}_0 = [\hat{\beta}_0^{\mathrm{re}}, \hat{\beta}_0^{\mathrm{im}}, \hat{x}_0]^{\mathrm{T}}$ by

$$\hat{x}_0 = \arg\max_{\hat{x}\in\mathcal{X}} \left|\mathbf{a}(\hat{x})^{\mathrm{H}}\tilde{\mathbf{W}}\tilde{\mathbf{y}}\right|, \hat{\beta}_0 = \left[\tilde{\mathbf{W}}^{\mathrm{H}}\mathbf{a}(\hat{x}_0)\right]^{+}\tilde{\mathbf{y}}, \quad (11)$$

where $\tilde{\mathbf{y}} = [\tilde{y}_1,\ldots,\tilde{y}_M]^{\mathrm{T}}$, $\tilde{\mathbf{W}} = [\tilde{\mathbf{w}}_1,\ldots,\tilde{\mathbf{w}}_M]$, $\mathcal{X} = \left\{\frac{1-M_0}{M_0}, \frac{3-M_0}{M_0}, \ldots, \frac{M_0-1}{M_0}\right\}$, the size $M_0 (M_0 \geq M)$ of $\mathcal{X}$ determines the estimation resolution, and $\mathbf{X}^{+} \triangleq (\mathbf{X}^{\mathrm{H}}\mathbf{X})^{-1}\mathbf{X}^{\mathrm{H}}$.

2) Beam and Channel Tracking: In time-slot n, two pilots are received at the beginning (see Fig. 3) using beamforming vectors $\mathbf{w}_{n,1}$ and $\mathbf{w}_{n,2}$, given by

$$\mathbf{w}_{n,1} = \frac{\mathbf{a}(\hat{x}_{n-1} - \delta^*)}{\sqrt{M}}, \ \mathbf{w}_{n,2} = \frac{\mathbf{a}(\hat{x}_{n-1} + \delta^*)}{\sqrt{M}}, \quad (12)$$

and the estimate $\hat{\boldsymbol{\psi}}_n = [\hat{\beta}_n^{\mathrm{re}}, \hat{\beta}_n^{\mathrm{im}}, \hat{x}_n]^{\mathrm{T}}$ is updated by (13) on the top of the page, where $\hat{\mathbf{g}}_n = \mathbf{W}_n^{\mathrm{H}}\mathbf{a}(\hat{x}_{n-1})$, $\hat{\mathbf{e}}_n = \hat{\beta}_{n-1}\mathbf{W}_n^{\mathrm{H}}\dot{\mathbf{a}}(\hat{x}_{n-1})$, $l_n = \|\hat{\mathbf{g}}_n\|_2\|\hat{\mathbf{e}}_n\|_2$, and $c_n = \hat{\mathbf{g}}_n^{\mathrm{H}}\hat{\mathbf{e}}_n$.

In *Stage 1*, the exhaustive sweeping is used, and the initial estimate $\hat{\boldsymbol{\psi}}_0$ is obtained in (11) by using the orthogonal matching pursuit method (e.g., [13]). This ensures that the initial beam direction $\hat{x}_0$ is within the mainlobe set, i.e.,

$$\mathcal{B}(x_0) \triangleq \left(x_0 - \frac{\lambda}{Md}, x_0 + \frac{\lambda}{Md}\right). \quad (14)$$

In *Stage 2*, the recursive tracker is motivated by the following maximization likelihood problem:

$$\max_{\hat{\boldsymbol{\psi}}_n}\left\{\max_{\mathbf{W}_n}\sum_{i=1}^{n}\mathbb{E}\left[\log p\left(\mathbf{y}_i|\hat{\boldsymbol{\psi}}_n,\mathbf{W}_i\right)\middle|\begin{matrix}\hat{\boldsymbol{\psi}}_n,\mathbf{W}_1,\ldots,\mathbf{W}_i,\\ \mathbf{y}_1,\ldots,\mathbf{y}_{i-1}\end{matrix}\right]\right\}, \quad (15)$$

where $\mathbf{W}_n = [\mathbf{w}_{n,1},\mathbf{w}_{n,2}]$ is subject to (2). We propose a two-layer nested optimization algorithm to find the solution of (15). In the *outer layer*, we use the stochastic Newton's method to update the estimate $\hat{\boldsymbol{\psi}}_n$, given by [19]

$$\hat{\boldsymbol{\psi}}_n = \hat{\boldsymbol{\psi}}_{n-1} - a_n\mathbb{E}\left[\mathbf{H}(\hat{\boldsymbol{\psi}}_{n-1},\mathbf{W}_n)\right]^{-1} \cdot \frac{\partial \log p(\mathbf{y}_n|\hat{\boldsymbol{\psi}}_{n-1},\mathbf{W}_n)}{\partial \hat{\boldsymbol{\psi}}_{n-1}}$$

$$= \hat{\boldsymbol{\psi}}_{n-1} + a_n\mathbf{I}(\hat{\boldsymbol{\psi}}_{n-1},\mathbf{W}_n)^{-1} \cdot \frac{\partial \log p(\mathbf{y}_n|\hat{\boldsymbol{\psi}}_{n-1},\mathbf{W}_n)}{\partial \hat{\boldsymbol{\psi}}_{n-1}}, \quad (16)$$

where $\mathbf{H}(\hat{\boldsymbol{\psi}}_{n-1},\mathbf{W}_n) = \frac{\partial^2 \log p(\mathbf{y}_n|\hat{\boldsymbol{\psi}}_{n-1},\mathbf{W}_n)}{\partial \hat{\boldsymbol{\psi}}_{n-1}\partial \hat{\boldsymbol{\psi}}_{n-1}^{\mathrm{T}}}$ is the Hessian matrix, $\mathbf{I}(\hat{\boldsymbol{\psi}}_{n-1},\mathbf{W}_n)$ can be calculated by using (7), a_n is the step-size that will be specified later, and

$$\frac{\partial \log p(\mathbf{y}_n|\hat{\boldsymbol{\psi}}_{n-1},\mathbf{W}_n)}{\partial \hat{\boldsymbol{\psi}}_{n-1}} = -\frac{2}{\sigma_0^2}\begin{bmatrix}\mathrm{Re}\{s^{\mathrm{H}}\hat{\mathbf{g}}_n^{\mathrm{H}}(\mathbf{y}_n - s\hat{\beta}_{n-1}\hat{\mathbf{g}}_n)\} \\ \mathrm{Im}\{s^{\mathrm{H}}\hat{\mathbf{g}}_n^{\mathrm{H}}(\mathbf{y}_n - s\hat{\beta}_{n-1}\hat{\mathbf{g}}_n)\} \\ \mathrm{Re}\{s^{\mathrm{H}}\hat{\mathbf{e}}_n^{\mathrm{H}}(\mathbf{y}_n - s\hat{\beta}_{n-1}\hat{\mathbf{g}}_n)\}\end{bmatrix}, \quad (17)$$

with $\hat{\mathbf{g}}_n = \mathbf{W}_n^{\mathrm{H}}\mathbf{a}(\hat{x}_{n-1})$ and $\hat{\mathbf{e}}_n = \hat{\beta}_{n-1}\mathbf{W}_n^{\mathrm{H}}\dot{\mathbf{a}}(\hat{x}_{n-1})$. Plugging $\mathbf{I}(\hat{\boldsymbol{\psi}}_{n-1},\mathbf{W}_n)$ and (17) in (16), we get (13). In the *inner layer*, it is equivalent to minimize the CRLB to update $\mathbf{W}_n$, i.e.,

$$\min_{\mathbf{W}_n}\left[\mathbf{I}(\hat{\boldsymbol{\psi}}_{n-1},\mathbf{W}_n)^{-1}\right]_{3,3}, \quad (18)$$

which results in (12).

Remark. *Different from the beam tracking algorithm in [17, 18], the RBCT algorithm uses two pilots and jointly updates the beam direction and channel coefficient in each time-slot.*

5. ASYMPTOTIC OPTIMALITY ANALYSIS

There are multiple stable points for (13), which correspond to the local optimal estimates for Problem (5) [21]. Hence Problem (5) is non-convex for the estimate $\hat{\boldsymbol{\psi}}_n$. To study these stable points, we rewrite (13) as follows:

$$\hat{\boldsymbol{\psi}}_n = \hat{\boldsymbol{\psi}}_{n-1} + a_n\left(\mathbf{f}\left(\hat{\boldsymbol{\psi}}_{n-1},\boldsymbol{\psi}_n\right) + \hat{\mathbf{z}}_n\right), \quad (19)$$

where $\mathbf{f}\left(\hat{\boldsymbol{\psi}},\boldsymbol{\psi}_n\right) \triangleq \mathbb{E}\left[\mathbf{I}(\hat{\boldsymbol{\psi}},\mathbf{W}_n)^{-1} \cdot \frac{\partial \log p(\mathbf{y}_n|\hat{\boldsymbol{\psi}},\mathbf{W}_n)}{\partial \hat{\boldsymbol{\psi}}}\middle|\boldsymbol{\psi}_n\right]$, and $\hat{\mathbf{z}}_n \triangleq \mathbf{I}(\hat{\boldsymbol{\psi}}_{n-1},\mathbf{W}_n)^{-1} \cdot \frac{\partial \log p(\mathbf{y}_n|\hat{\boldsymbol{\psi}}_{n-1},\mathbf{W}_n)}{\partial \hat{\boldsymbol{\psi}}_{n-1}} - \mathbf{f}\left(\hat{\boldsymbol{\psi}}_{n-1},\boldsymbol{\psi}_n\right)$.

A stable point $\hat{\boldsymbol{\psi}}_{n-1}$ should satisfy: $\mathbf{f}\left(\hat{\boldsymbol{\psi}}_{n-1},\boldsymbol{\psi}_n\right) = \mathbf{0}$, and $\frac{\partial \mathbf{f}(\hat{\boldsymbol{\psi}}_{n-1},\boldsymbol{\psi}_n)}{\partial \hat{\boldsymbol{\psi}}_{n-1}^{\mathrm{T}}}$ is a negative definite matrix. Let $\mathcal{S}_n$ denote the stable points set at time-slot n. Then, we can verify $\boldsymbol{\psi}_n \in \mathcal{S}_n$, whose details are given in our technical report [22].

Note that except for the real direction x_n, the antenna array gain is quite low at other local optimal stable points in $\mathcal{S}_n$. Hence, one key challenge is *how to ensure that the RBCT algorithm converges to the real direction x_n, instead of other local optimal stable points in $\mathcal{S}_n$.*

In *static* beam tracking, where $\boldsymbol{\psi}_n = \boldsymbol{\psi} = [\beta^{\mathrm{re}},\beta^{\mathrm{im}},x]^{\mathrm{T}}$ and $\mathcal{S}_n = \mathcal{S}$, we adopt the diminishing step-sizes [19, 21, 23]:

$$a_n = \frac{\alpha}{n+N_0}, \ n = 1,2,\ldots, \quad (20)$$

where $\alpha > 0$ and $N_0 \geq 0$. We use the stochastic approximation and recursive estimation theory [19, 21, 23] to analyze the RBCT algorithm. To support the more general joint beam and channel tracking scenario than [17, 18], three new theorems are developed to resolve the challenge mentioned above:

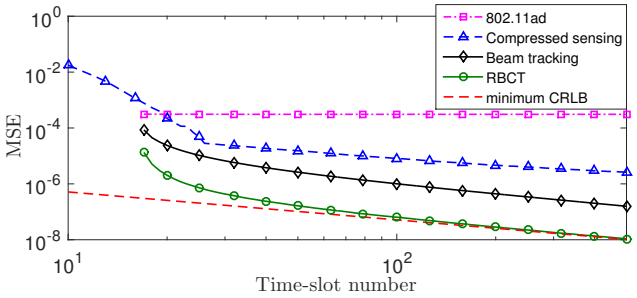

Fig. 4. MSE vs. time-slot number in static scenarios.

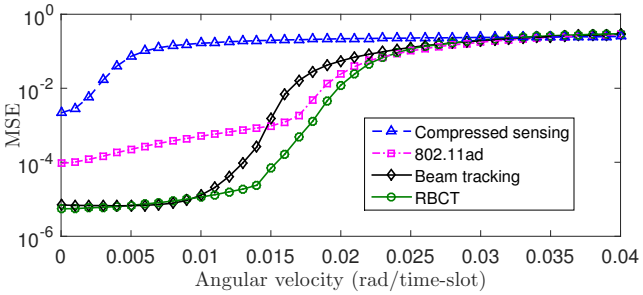

Fig. 5. MSE vs. angular velocity in dynamic scenarios.

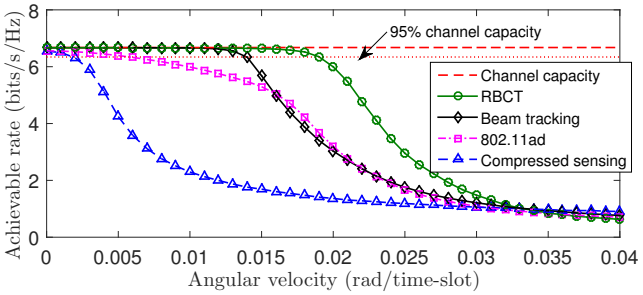

Fig. 6. Data rate vs. angular velocity in dynamic scenarios.

Theorem 1 (**Convergence to Stable Points**). *If a_n is given by (20) with any $\alpha > 0$ and $N_0 \geq 0$, then $\hat{\psi}_n$ converges to a unique point within $\mathcal{S}$ with probability one.*

Hence, for general step-size parameters α and N_0 in (20), $\hat{x}_n$ converges to a stable point in $\mathcal{S}$.

Theorem 2 (**Convergence to the Real Beam Direction** x). *If (i) $\hat{x}_0 \in \mathcal{B}(x)$, (ii) a_n is given by (20) with any $\alpha > 0$, then there exist $N_0 \geq 0$ and $C > 0$ such that*

$$P\left(\hat{x}_n \to x \middle| \hat{x}_0 \in \mathcal{B}(x)\right) \geq 1 - 6e^{-\frac{C|s|^2}{\alpha^2\sigma_0^2}}. \quad (21)$$

By Theorem 2, if the initial point $\hat{x}_0$ is in the mainlobe $\mathcal{B}(x)$, the probability that $\hat{x}_n$ does not converge to x decades *exponentially* with respect to $\frac{|s|^2}{\alpha^2\sigma_0^2}$. Hence, one can increase the transmit SNR $\frac{|s|^2}{\sigma_0^2}$ and reduce the step-size parameter α to ensure $\hat{x}_n \to x$ with high probability.

Theorem 3 (**Convergence to x with the Minimum MSE**). *If (i) a_n is given by (20) with $\alpha = 1$ and any $N_0 \geq 0$, and (ii) $\hat{\psi}_n \to \psi$, then*

$$\lim_{n\to\infty} n\mathbb{E}\left[(\hat{x}_n - x)^2 \middle| \hat{\psi}_n \to \psi\right] = \left[\mathbf{I}(\psi, \mathbf{W}^*)^{-1}\right]_{3,3}. \quad (22)$$

Theorem 3 tells us that α should not be too small: If $\alpha = 1$, then the minimum CRLB on the RHS of (8) is achieved asymptotically with high probability.

Proof description of Theorem 1-3. The main difference from [17, 18] is that the RBCT algorithm considers vector variable/function rather than the scalar ones in [17, 18]. Hence, the main proof structures are similar, while the parts that involve these vectors are different. Due to space limitation, the detailed proofs are provided in our technical report [22]. □

6. NUMERICAL RESULTS

We compare the RBCT algorithm with three reference algorithms: the compressed sensing algorithm [13], the IEEE 802.11ad algorithm [14], and the beam tracking algorithm [18]. The first two algorithms have the same configuration as that in Section VI of [18]. The third one uses the same training beamforming vectors as the RBCT algorithm, i.e., in each time-slot, it receives two pilots with the beamforming vectors in (12), and the beam direction is tracked by using both observations. Moreover, its channel coefficient is obtained with a least square estimator by using these observations. Consider the system model in Section 2 with $M = 32$ antennas, and the antenna spacing is $d = 0.5\lambda$. The pilot symbol is $s = \frac{1+j}{2}$, and the transmit SNR $\frac{|s|^2}{\sigma^2}$ is set as 5dB. To ensure fairness, we assume that 2 pilot symbols are received in each time-slot, hence all the algorithms have the same pilot overhead.

In static scenarios, we set the step-size as $a_n = \frac{1}{n}, n \geq 1$. The real AoA θ is randomly generated by a uniform distribution on $[-90°, 90°]$ in each realization, and the results are averaged over 10000 random realizations. Figure 4 plots the MSE over time. It can be observed that the MSE of the RBCT algorithm converges to the minimum CRLB in (8), which is much smaller than the reference algorithms.

In dynamic scenarios, we set the step-size as a constant value, i.e., $a_n = 1, n \geq 1$. The channel variation is modeled as: The AoA $\theta_n = \theta_{n-1} + \delta_{n-1} \cdot \omega$ where $\theta_0 = 0$, $\delta_n \in \{-1, 1\}$ denotes the rotation direction, and $\omega \in [0, 0.04]$ is a fixed angular velocity. The rotation direction δ_n is chosen such that θ_n varies within $[-\frac{\pi}{3}, \frac{\pi}{3}]$. The channel coefficient $\beta_n (\mathbb{E}\left[|\beta_n|^2\right] = 1)$ is subject to Rician fading with a K-factor $\kappa = 15$dB, according to the channel model proposed in [24]. In Fig. 5 and 6, one can observe that the RBCT algorithm can support much higher angular velocities and data rates than other algorithms. According to Fig. 6, the RBCT algorithm can achieve 95% of channel capacity when the angular velocity is 0.19rad (1.09 degrees) per time-slot. If 5 time-slots last for one second, i.e., 10 pilots per second received, then the RBCT algorithm is capable of tracking a mobile moving at an angular velocity of 5.45 degrees per second and achieving over 95% of channel capacity.

7. CONCLUSION

We have developed a joint beam and channel tracking algorithm for mmWave phased antenna arrays, and established its convergence and asymptomatic optimality. Our simulation results show that the proposed algorithm can achieve much faster tracking speed, lower beam tracking error, and higher data rate than several state-of-the-art algorithms, with the same pilot overhead.

8. REFERENCES

[1] Z. Pi and F. Khan, "An introduction to millimeter-wave mobile broadband systems," *IEEE Commun. Mag.*, vol. 49, no. 6, Jun. 2011.

[2] F. Boccardi, R. W. Heath, A. Lozano, T. L. Marzetta, and P. Popovski, "Five disruptive technology directions for 5G," *IEEE Commun. Mag.*, vol. 52, no. 2, Feb. 2014.

[3] R. W. Heath, N. González-Prelcic, S. Rangan, W. Roh, and A. M. Sayeed, "An overview of signal processing techniques for millimeter wave MIMO systems," *IEEE J. Sel. Top. Signal Process.*, Apr. 2016.

[4] T. S. Rappaport, S. Sun, R. Mayzus, H. Zhao, Y. Azar, K. Wang, G. N. Wong, J. K. Schulz, M. Samimi, and F. Gutierrez, "Millimeter wave mobile communications for 5G cellular: it will work!," *IEEE Access*, vol. 1, May 2013.

[5] T. S. Rappaport, G. R. MacCartney, M. K. Samimi, and S. Sun, "Wideband millimeter-wave propagation measurements and channel models for future wireless communication system design," *IEEE Trans. Commun.*, vol. 63, no. 9, Sep. 2015.

[6] S. Sun, T. S. Rappaport, R. W. Heath, A. Nix, and S. Rangan, "MIMO for millimeter-wave wireless communications: Beamforming, spatial multiplexing, or both?," *IEEE Commun. Mag.*, vol. 52, no. 12, Dec. 2014.

[7] S. Han, C. L. I, Z. Xu, and C. Rowell, "Large-scale antenna systems with hybrid analog and digital beamforming for millimeter wave 5G," *IEEE Commun. Mag.*, vol. 53, no. 1, Jan. 2015.

[8] A. Puglielli, A. Townley, G. LaCaille, V. Milovanovi, P. Lu, K. Trotskovsky, A. Whitcombe, N. Narevsky, G. Wright, T. Courtade, E. Alon, B. Nikoli, and A. M. Niknejad, "Design of energy- and cost-efficient massive MIMO arrays," *Proc. IEEE*, vol. 104, no. 3, Mar. 2016.

[9] A. F. Molisch, V. V. Ratnam, S. Han, Z. Li, S. L. H. Nguyen, L. Li, and K. Haneda, "Hybrid beamforming for massive MIMO-a survey," *IEEE Commun. Mag.*, vol. 55, no. 9, Sep. 2017.

[10] Gabriel Brown, Ozge Koymen, and Matt Branda, "The promise of 5G mmWave - How do we make it mobile?," *Qualcomm Technologies*, Jun. 2016.

[11] Junyi Wang, Zhou Lan, Chang-Woo Pyo, Tuncer Baykas, Chin-Sean Sum, M Azizur Rahman, Jing Gao, Ryuhei Funada, Fumihide Kojima, Hiroshi Harada, and Shuzo Kato, "Beam codebook based beamforming protocol for multi-Gbps millimeter-wave WPAN systems," *IEEE J. Sel. Areas Commun.*, vol. 27, no. 8, Oct. 2009.

[12] A. Alkhateeb, O. El Ayach, G. Leus, and R. W. Heath, "Channel estimation and hybrid precoding for millimeter wave cellular systems," *IEEE J. Sel. Top. Signal Process.*, vol. 8, no. 5, Oct. 2014.

[13] A. Alkhateeb, G. Leusz, and R. W. Heath, "Compressed sensing based multi-user millimeter wave systems: How many measurements are needed?," in *IEEE ICASSP*, Apr. 2015.

[14] IEEE standard, "IEEE 802.11ad WLAN enhancements for very high throughput in the 60 GHz band," Dec. 2012.

[15] Joan Palacios, Danilo De Donno, and Joerg Widmer, "Tracking mm-Wave channel dynamics: Fast beam training strategies under mobility," *IEEE INFOCOM*, 2017.

[16] X. Gao, L. Dai, Y. Zhang, T. Xie, X. Dai, and Z. Wang, "Fast channel tracking for Terahertz beamspace massive MIMO systems," *IEEE Trans. Veh. Technol.*, vol. 66, no. 7, Jul. 2017.

[17] J. Li, Y. Sun, L. Xiao, S. Zhou, and C. E. Koksal, "Analog beam tracking in linear antenna arrays: Convergence, optimality, and performance," in *51st Asilomar Conference on Signals, Systems, and Computers*, 2017.

[18] J. Li, Y. Sun, L. Xiao, S. Zhou, and C. E. Koksal, "Super fast beam tracking in phased antenna arrays," *arXiv preprint arXiv:1710.07873*, 2017.

[19] M. B. Nevel'son and R. Z. Has'minskii, *Stochastic approximation and recursive estimation*, 1973.

[20] H. V. Poor, *An introduction to signal detection and estimation*, Springer-Verlag New York, Inc., New York, NY, USA, 1994.

[21] H. Kushner and G. G. Yin, *Stochastic approximation and recursive algorithms and applications*, vol. 35, Springer Science & Business Media, 2003.

[22] J. Li, Y. Sun, L. Xiao, S. Zhou, and A. Sabharwal, "How to mobilize mmwave: A joint beam and channel tracking approach," *technical report, arXiv preprint arXiv:1802.02125*, 2018.

[23] V. S. Borkar, *Stochastic approximation: a dynamical systems viewpoint*, 2008.

[24] M. K. Samimi, G. R. MacCartney, S. Sun, and T. S. Rappaport, "28GHz millimeter-wave ultrawideband small-scale fading models in wireless channels," in *2016 IEEE VTC Spring*, May 2016.